Article ID: 1007-4627(2012)01-0036-09

Transverse Mass Spectra in High-energy Heavy-ion Collisions

XIE Wen-jie

(*Department of Physics, Yuncheng University, Yuncheng* 044000, *Shanxi, China*)

Abstract: Based on the multisource ideal gas model, which do not consider the dynamic mechanism of particles, two formulae are given to describe the transverse mass distributions of protons, kaons and pions produced in central heavy ion collisions at high energies. In the case of neglecting the relativistic effect, our calculated results approximately describe the experimental data, except for pions. By considering the sub-samples of the sources, it is found that our calculated results are in good agreement with the experimental data in the central Au-Au and Pb-Pb collisions at high energies.

Key words: multisource ideal gas model; transverse mass spectrum; Au-Au collision; Pb-Pb collision

CLC number: O571.6 **Document code**: A

1 Introduction

The study of high-energy heavy-ion interactions is an important field of particle and nuclear physics and it is motivated mainly by the quantum chromodynamics (QCD) prediction that the excited nuclear matter undergoes a phase transition into a system of deconfined quarks and gluons under extremely high temperature and high density[1].

In the study of relativistic heavy-ion collisions, the transverse mass (m_T) distributions of final-state particles are the interesting subject in theoretical and experimental investigations. Many international collaborations have reported the m_T distributions of final-state particles, for instance, E895[2], E917[3], NA49[4−12], NA57[13], E802[14], E866 and E917[15], etc.. Meanwhile, much theoretical work has been devoted to the understanding of the mechanism responsible for the m_T distributions[16−20].

Recently, based on the multisource ideal gas (MSIG) model[21−28], Liu et al. have given a unified description to multiplicity distributions of the final-state particles measured in e^+e^-, pp, $p\bar{p}$, e^+p and proton and heavy ion induced nuclear collisions at different center-of-mass energies[21], and $^{56}Fe+p$, ^{136}Xe (^{124}Xe)$+Pb$ reactions over an energy range from 300 to 1500 *A*MeV[22]. It is known that the MSIG model is successful in describing rapidity and azimuthal distributions of protons produced in the Au-Au collisions at 2 ∼ 8 *A*GeV measured at alternating-gradient synchrotron (AGS)[23]. In our previous work[29−30], we have used the three-fireball model to describe the m_T distributions of strange particles produced in the Pb-Pb collisions at 40, 80 and 158 *A*GeV. To study other particle productions in a wider energy range, in this paper we develop the methods used

Received date: 2 Mar. 2011; **Revised date**: 17 Apr. 2011

Foundation item: National Natural Science Foundation of China(10975095); Natural Science Foundation of Shanxi Province (2007011005)

Biography: XIE Wen-jie(1980—), male, Yuncheng, Shanxi, China, Master, working on the field of high energy physics;
E-mail: wenjiexie@yeah.net

in the Refs. [29－30] to calculate the m_T distributions of protons, kaons, pions, lambda and antilambda and compare with the experimental data in the range from alternating-gradient synchrotron (AGS) to super proton synchrotron (SPS) incident energies.

2 The MSIG model

We establish a three-dimensional rectangular coordinate system and let the beam direction and the reaction plane be the oz axis and xoz plane respectively. In the MISG model, many emission sources of particles are assumed to form in heavy-ion collisions at high energies. A lot of particles are produced and emitted in each emission source. We assume that the particles are isotropically emitted in the rest frame of emission source. According to Ref. [28], the m_T distribution of particles produced in the emission source i is given by

$$f_i(m_T, T_i) = Cm_T \exp\left(-\frac{m_T^2 - m_0^2}{2m_0 T_i}\right), \quad (1)$$

where C is the normalization constant, m_0 is the rest mass of the concerned particle, and T_i is the temperature parameter which describes the excitation degree of the ith emission source. The final m_T distribution, contributed by all n emission sources, is

$$f(m_T) = \sum_{i=1}^{n} a_i f_i(m_T, T_i), \quad (2)$$

where a_i is the relative weight contributed by the ith emission source. As a raw assumption, all n emission sources are in thermal and chemical equilibrium at the time of freeze-out. We have

$$T_1 = T_2 = \cdots = T_n. \quad (3)$$

In present paper we assume

$$a_1 = a_2 = \cdots = a_n. \quad (4)$$

We would like to point out that Eq. (1) is valid only in the non-relativistic limit. In the laboratory reference frame, the concerned particles of the present work are not non-relativistic. But in the emission source rest frame the relativistic effect is small. In fact, when the particles in the laboratory system are transformed into the one in the emission source rest system we can use Eq. (1) to describe the transverse mass spectra of both the non-relativistic and relativistic particles. However, the transforming work is too complex to realize in the present work. Therefore, as a first approximation, Eq. (1) is used in this paper. In the case of considering relativistic particles, we can use the method in the following.

In high-energy heavy-ion collisions, according to the interaction mechanisms or event sample, many emission sources formed in high-energy heavy-ion collisions are divided into l groups[21－22]. The source number in the jth group is assumed to be n_j. Each source contributes m_T distribution to be an exponential function.

The transverse mass (m_{Tij}) distribution contributed by the ith source in the jth group is written as

$$f_{ij}(m_{Tij}, T_{ij}) = \frac{1}{T_{ij}} \exp\left(-\frac{m_{Tij}}{T_{ij}}\right), \quad (5)$$

where T_{ij} is the temperature of the ith emission source in the jth group. We assume that the emission sources in the jth group are in thermal and chemical equilibrium at the time of freeze-out. We have

$$T_{1j} = T_{2j} = \cdots = T_{n_j j}. \quad (6)$$

The particle transverse mass (m_{Tj}) distribution contributed by the jth group is given by the folding of n_j exponential functions, that is

$$f_j(m_{Tj}, T_{ij}) = \frac{m_{Tj}^{n_j - 1}}{(n_j - 1)!\ T_{ij}^{n_j}} \exp\left(-\frac{m_{Tj}}{T_{ij}}\right). \quad (7)$$

The total m_T distribution contributed by the l groups can be written as

$$f(m_{Tj}, T_{ij}) = \sum_{j=1}^{l} b_j f_j(m_{Tj}, T_{ij}), \quad (8)$$

where b_j is the relative weight contributed by the jth group and can be obtained by the geometrical

weight of the impact parameter. A greater geometrical weight of the impact parameter corresponds to a greater value of b_j. For nucleus-nucleus collisions at a fixed impact parameter, the n_j can be regarded as the number of participant nuclei. For nucleus-nucleus collisions at a random impact parameter, the number of participant nuclei will be various. Going further, the m_T will be various. The m_T distribution is finally obtained by the statistical method. In Ref. [16], for instance, the m_T distribution of the protons produced in the Pb-Pb collisions at incident energies $E_{lab}=158$, 80, 40, 30 and 20 AGeV, the three-fluid dynamics(3FD) model has used a fixed impact parameter to describe the experimental data. It is different from the present work.

In the above discussions, two methods in the framework of the MSIG model are proposed to describe the m_T distributions. For the first method, all of the emission sources formed in high-energy heavy-ion collisions are assumed to be in thermal and chemical equilibrium at the time of freeze-out. Then, the temperatures of all the emission sources are the same. For the second method, the emission sources formed in high-energy heavy-ion collisions are divided into l groups accor-ding to interaction mechanisms or event sample. We assume that all the emission sources in each group are in thermal and chemical equilibrium at the time of freeze-out. All the groups are not always in thermal and chemical equilibrium. Therefore, the temperatures of all the emission sources in each group are same and the temperatures of the emission sources in different groups are not always the same.

In addition, Eq. (5) in this paper are different from Eq. (2) in Ref. [13]. Eq. (2) of Ref. [13] is the parametrization for each particle species and Eq. (5) in this paper is the contribution of each emission source including the various particles. Also the temperature parameter used in the present work is different from the temperature parameter used in Ref. [13]. The temperature of the present work is used to describe the excitation degree of the emission source and the temperature of Ref. [13] is interpreted as due to the thermal motion coupled with a collective transverse flow of the fireball components.

3 Comparison with experimental data

The m_T spectra, $(1/m_T)d^2N/dydm_T$, of protons at the midrapidity produced in the central Au-Au collisions at the different AGS energies and in the central Pb-Pb collisions at the different SPS energies are represented in Figs. 1 and 2 respectively, where N and y denote particle number and rapidity respectively. The circles denote the experimental data of the E895 Collaboration[2]

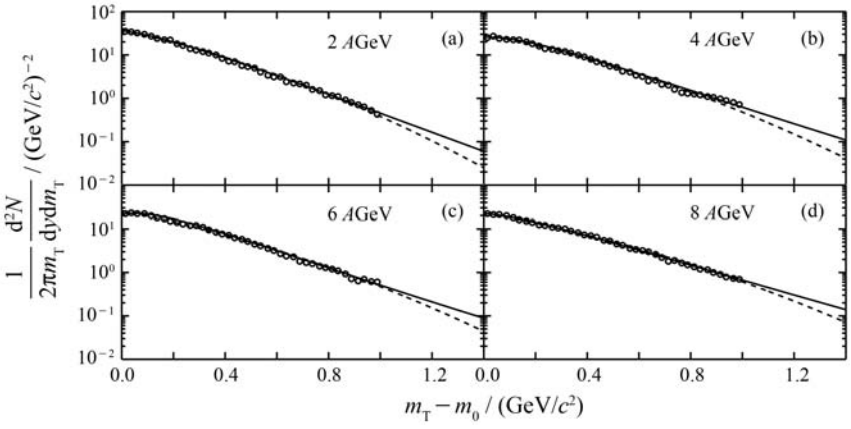

Fig. 1 The transverse mass distributions of protons at the midrapidity from the central Au-Au collisions at incident energies $E_{lab}=2$, 4, 6 and 8 AGeV. Data are from the E895 experimental data[2].

and NA49 experimental data[4−6]. The dashed curves are our calculated results using Eq. (2) and the solid curves are the calculated results with Eq. (8) with $j=2$. From 2 to 8 AGeV, the T_i values by fitting the experimental data with Eq. (2), the T_{ij}, n_j values and the relationship of b_1 and b_2 in Eq. (8) are shown in Table 1. In the selection of the parameter values, the χ^2-testing method is used and the χ^2/dof (dof means degree of freedom) values are shown in Table 1. It can be seen that Eq. (2) and (8) describe the experimental data well, there is no obvious difference between Eq. (2) and (8) in describing the m_T spectra of the protons from the central Au-Au collisions at the AGS incident energies and the central Pb-Pb collisions at the SPS incident energies.

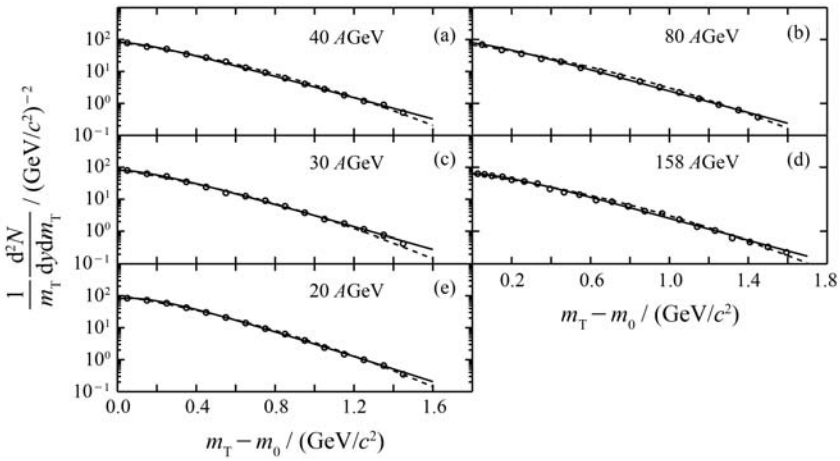

Fig. 2 The transverse mass distributions of protons at the midrapidity from central Pb-Pb collisions at incident energies E_{lab} = 20, 30, 40, 80 and 158 AGeV. Data are taken from the NA49 Collaboration[4−6].

Table 1 The T_i values of Eq. (2), the T_{ij}, n_j values and the relations between b_1 and b_2 in Eq. (8) for Figs. 1～3.

	Incident energy/(AGeV)	T_i /GeV	$f(b_1, b_2)$	T_{i1} /GeV	T_{i2} /GeV	n_1	n_2	$\frac{\chi^2}{\text{dof}}$
Fig. 1	2	0.33	$b_1 = 2.1b_2$	0.21	0.15	2	3	0.074
	4	0.37	$b_1 = 1.8b_2$	0.25	0.15	2	3	0.099
	6	0.38	$b_1 = 1.6b_2$	0.25	0.14	2	3	0.101
	8	0.42	$b_1 = 3.5b_2$	0.27	0.16	2	3	0.042
Fig. 2	20	0.45	$b_1 = 0.8b_2$	0.245	0.175	2	3	0.041
	30	0.46	$b_1 = 1.8b_2$	0.27	0.18	2	3	0.064
	40	0.49	$b_1 = 2.3b_2$	0.28	0.18	2	3	0.083
	80	0.49	$b_1 = 4.0b_2$	0.27	0.18	2	3	0.025
	158	0.51	$b_1 = 2.3b_2$	0.28	0.18	2	3	0.065
Fig. 3	2	0.23	$b_1 = b_2$	0.135	0.095	2	3	0.135
	4	0.26	$b_1 = b_2$	0.14	0.10	2	3	0.091
	6	0.31	$b_1 = 4.0b_2$	0.187	0.125	2	3	0.038
	8	0.32	$b_1 = 0.4b_2$	0.08	0.18	2	3	0.186
	10.7	0.37	$b_1 = 0.4b_2$	0.30	0.185	2	3	0.107

We show in Fig. 3 the m_T distributions, $(1/2\pi m_T)\,d^2N/dm_T dy$, of positive kaons at the midrapidity produced in the central Au-Au collisions at the various AGS incident energies. The circles denote the E866 experimental data[15]. The dashed curves are our calculated results using Eq. (2). The solid curves are the results from Eq. (8) with $j=2$ and the obtained parameter values by fitting the experimental data are shown in Table 1. From 2 to 10.7 AGeV, the obtained T_i

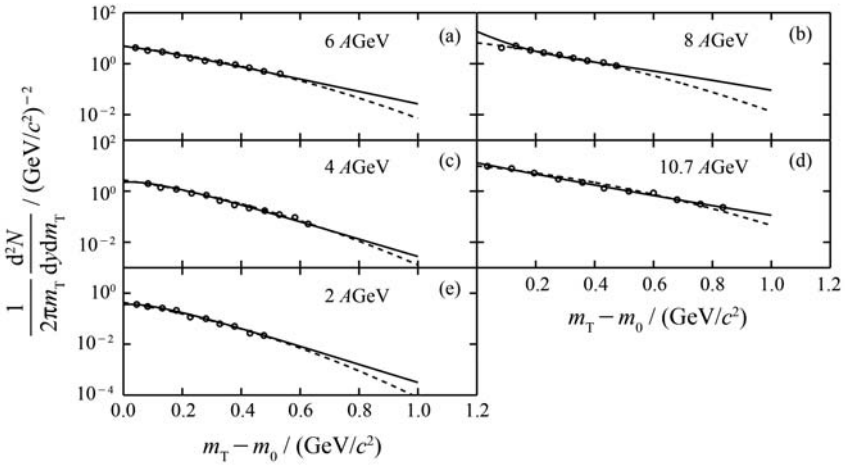

Fig. 3 The transverse mass distributions of positive kaons at the midrapidity from the central Au-Au collisions at incident energies E_{lab} = 2, 4, 6, 8 and 10.7 *A*GeV. The experimental data are from the E866 Collaboration[15].

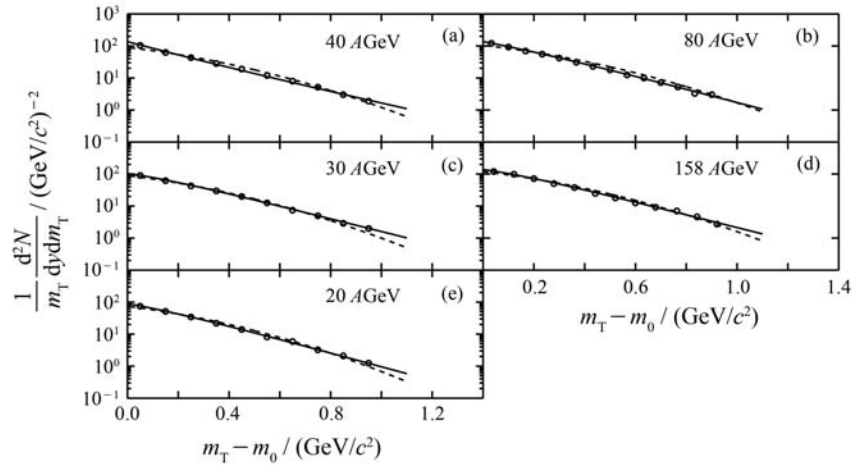

Fig. 4 The transverse mass distributions of positive kaons at the midrapidity from the central Pb-Pb collisions at incident energies E_{lab} = 20, 30, 40, 80 and 158 *A*GeV. The experimental data are taken from Ref. [16].

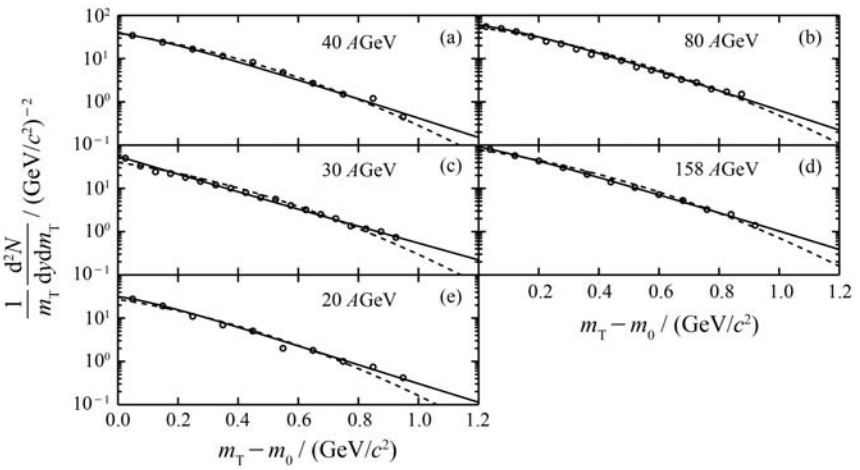

Fig. 5 The caption is the same as that for Fig. 4, but displays the results of negative kaons.

values of Eq. (2) and the relations between b_1 and b_2 in Eq. (8) are shown in Table 1. In the selection of parameter values, the χ^2-testing method is used and the χ^2/dof values are also shown in Table 1.

The m_T distributions, $(1/m_T)d^2N/dm_Tdy$, of positive and negative kaons at the midrapidity pro-

duced in the central Pb-Pb collisions at the different SPS incident energies are given respectively in Figs. 4 and 5. The circles denote the experimental data which are taken from Ref. [16]. The dashed curves represent our calculated results by using Eq. (2) and the solid curves indicate the results by using Eq. (8) with $j=2$ and the obtained parameter values by fitting the experimental data are shown in Table 2. The fitted T_i values of Eq. (2), the χ^2/dof values and the relationship of b_1 and b_2 are shown in Table 2. From Figs. 3, 4 and 5, we can see that Eq. (8) is better than Eq. (2) in the descriptions of the m_T distributions of kaons from the central heavy-ion collisions in the range from AGS to SPS incident energies.

The m_T distributions, $(1/2\pi m_T)d^2N/dm_T dy$,

Table 2　The T_i values of Eq. (2), the T_{ij}, n_j values and the relations between b_1 and b_2 in Eq. (8) for Figs. 4～7

	Incident energy/(AGeV)	T_i/GeV	$f(b_1, b_2)$	T_{i1}/GeV	T_{i2}/GeV	$n_1 v$	n_2	$\frac{\chi^2}{\text{dof}}$
Fig. 4	20	0.43		0.21	0.15	2	3	0.026
	30	0.45		0.23	0.15	2	3	0.062
	40	0.47	$b_1=4.0b_2$	0.25	0.16	2	3	0.037
	80	0.49		0.215	0.165	2	3	0.125
	158	0.49		0.23	0.15	2	3	0.11
Fig. 5	20	0.39	$b_1=4.0b_2$	0.21	0.13	2	3	0.406
	30	0.41	$b_1=4.0b_2$	0.23	0.17	2	2	0.06
	40	0.41	$b_1=2.3b_2$	0.204	0.15	2	3	0.317
	80	0.43	$b_1=1.8b_2$	0.20	0.15	2	3	0.069
	158	0.43	$b_1=4.0b_2$	0.21	0.16	2	3	0.039
Fig. 6	2	0.48	$b_1=9.0b_2$	0.10	0.092	2	5	0.581
	4	0.52	$b_1=2.8b_2$	0.10	0.10	2	5	0.411
	6	0.56	$b_1=2.0b_2$	0.10	0.10	2	5	0.403
	8	0.60	$b_1=1.2b_2$	0.10	0.15	2	3	0.032
	10.7	0.64	$b_1=1.2b_2$	0.105	0.155	2	3	0.058
Fig. 7	20	0.41	$b_1=4.0b_2$	0.12	0.105	2	5	0.115
	30	0.41	$b_1=3.8b_2$	0.13	0.13	2	5	0.085
	40	0.45	$b_1=3.3b_2$	0.13	0.13	2	5	0.056
	80	0.48	$b_1=3.3b_2$	0.12	0.13	2	5	0.102
	158	0.56	$b_1=3.8b_2$	0.13	0.13	2	3	0.234

of positive pions at the midrapidity produced in the central Au-Au collisions at the various AGS incident energies and $(1/m_T)d^2N/dm_T dy$, of negative pions at the midrapidity from the central Pb-Pb collisions at the different SPS incident energies are displayed in Figs. 6 and 7, respectively. The experimental data are taken from the E866 and E917 Collaborations[15] and the NA49 Collaboration[9-10], which are showed by the circles. The dashed curves show our calculated results from Eq. (2) and the solid curves show the calculated results from Eq. (8) with $j=2$. The fitted T_i values of Eq. (2), the fitted T_{ij}, n_j values and the relationship between b_1 and b_2 of Eq. (8) are shown in Table 2. In the selection of parameter values, the χ^2-testing method is used and the obtained χ^2/dof values are shown in Table 2. It can be seen from Figs. 6 and 7 that Eq. (8) is successful in describing the m_T distributions of pions produced in the central Au-Au collisions at the AGS incident energies and in the central Pb-Pb collisions at the SPS incident energies. We believe that the rough as-

sumption that all of sources are in thermal and chemical equilibrium at the time of freeze-out would be responsible for the unsuccessfulness of Eq. (2) in describing the m_T distributions of pions.

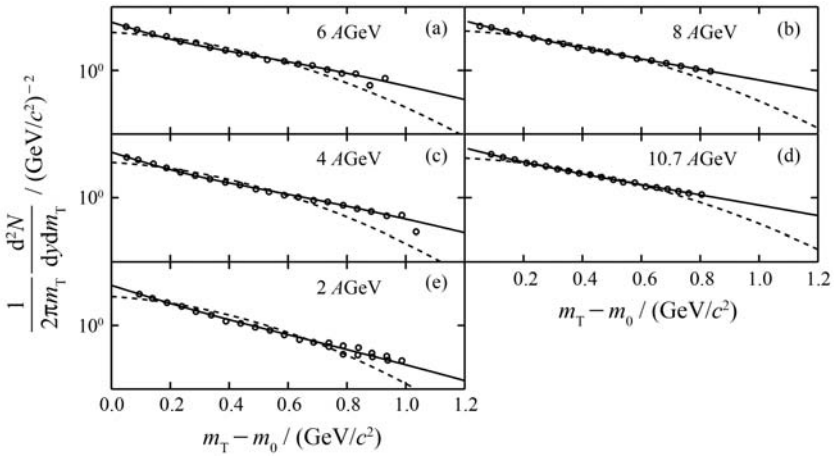

Fig. 6 The same as in Fig. 3 but for positive pions. Data are from the E866 and E917 Collaborations[15].

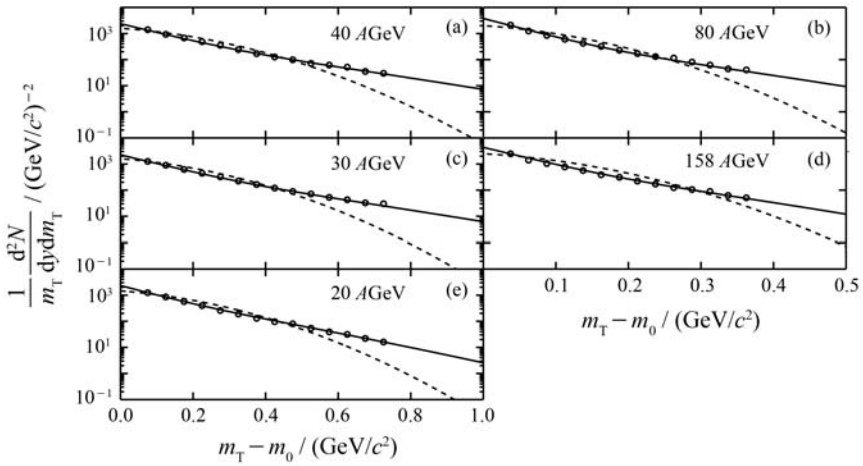

Fig. 7 The title is the same as that for Fig. 4, but indicates the results of negative pions. Experimental data are from the NA49 Collaboration[9-10].

4 Conclusions and discussions

We have used two methods, which are based on the MSIG model, to calculate the m_T distributions of the final-state particles produced in the heavy ion collisions at high energies. In the first method, we assume that all of the emission sources of the particles are in thermal and chemical equilibrium at the time of freeze-out. This assumption is similar to the one used in Refs. [29-30]. Although it is rough, we can use it to approximately describe the m_T distributions of the particles, except for pions. In Ref. [30], we described successfully the m_T distributions of strange particles produced in the Pb-Pb collisions at 40 and 158 *A*GeV by considering the expansion of emission source in the transverse direction, which is different from the first method used in the present work. In the second method, a formula which considers the jth sub-sample in the calculations is obtained to give a description of the m_T distributions of the final-state particles produced in the Au-Au and Pb-Pb collisions at the AGS and SPS incident energies. Compared with the first method, the

second method is better in describing the m_T distributions of the final-state particles, especially for pions.

A few modelling formulae are used in describing m_T distributions. For example, the exponential distributions[13, 16], the two exponential distributions[7−8], etc. Eq. (7) which has been used in the present work is actually an Erlang distribution. Generally speaking, for nucleus-nucleus collisions at not too high energies we take $j=1$ and for collisions at very high energies we take $j=2$ or 3 due to the different interaction mechanisms existing in the event samples. One can see that our modelling formula (Eq. (8)) includes the formulas in Refs. [6−7, 13, 16]. For the MSIG model, the distinction of distributions can be seen from the temperature of the emission source (T_i or T_{ij}) , the numbers of the group divided (l), the relative weight of the divided group (b_j) and the source numbers of each group (n_j).

In summary, the m_T distributions of the final-state particles produced in the central Au-Au collisions at the AGS energies and in the central Pb-Pb collisions at the SPS energies have been investigated by the multisource ideal gas model. Two formulas describing the m_T distributions are obtained. The model is proved to be successful in describing the final-state particle m_T distributions at the energy range concerned.

References:

[1] CABIBBO N, PARISI G. Phys Lett, 1975, **B59**: 67.

[2] KLAY J L, AJITANAND N N, ALEXANDER J M, *et al*. Phys Rev Lett, 2002, **88**: 102301.

[3] BACK B B, BETTS R R, CHANG J, *et al*. Phys Rev Lett, 2001, **86**: 1970.

[4] GAZDZICKI M, the NA49 Collaboration. J Phys, 2004, **G30**: S701.

[5] APPELSHÄUSER H, BÄCHLER J, BAILEY S J, *et al*. Phys Rev Lett, 1999, **82**: 2471.

[6] VAN L M, AFANASIEV S V, ANTICIC T, *et al*. Nucl Phys, 1999, **A715**: 161c.

[7] ANTICIC T, BAATAR B, BARNA D, *et al*. Phys Rev, 2004, **C69**: 024902.

[8] ALT C, ANTICIC T, BAATAR B, *et al*. Phys Rev, 2006, **C73**: 044910.

[9] AFANASIEV S V, ANTICIC T, BARNA D, *et al*. Phys Rev, 2002, **C66**: 054902.

[10] ALT C, ANTICIC T, BAATAR B, *et al*. J Phys, 2004, **G30**: S119.

[11] ANTICIC T, BAATAR B, BARNA D, *et al*. Phys Rev Lett, 2004, **93**: 022302.

[12] ANTICIC T, BAATAR B, BARNA D, *et al*. Phys Rev, 2009, **C80**: 034906.

[13] ANTINORI F, BACON P, BADALÁ A, *et al*. J Phys, 2004, **G30**: 823.

[14] AHLE L, AKIBA Y, ASHKTORAB K, *et al*. Phys Rev, 1999, **C59**: 2173.

[15] AHLE L, AKIBA Y, ASHKTORAB K, *et al*. Phys Lett, 2000, **B476**: 1.

[16] IVANOV Y B, RUSSKIKH V N. Phys Rev, 2008, **C78**: 064902.

[17] WAGNER M, LARIONOV A B, MOSEL U. Phys Rev, 2005, **C71**: 034910.

[18] BRATKOVSKAYA E L, SOFF S, STOECKER H, *et al*. Phys Rev Lett, 2004, **92**: 032302.

[19] BRATKOVSKAYA E L, BLEICHER M, REITER M, *et al*. Phys Rev, 2004, **C69**: 054907.

[20] GAZDZICKI M, GORENSTEIN M I, GRASSI F, *et al*. Braz J Phys, 2004, **34**: 322.

[21] LIU F H. Nucl Phys, 2008, **A810**: 159.

[22] LIU F H, LI J S. Phys Rev, 2008, **C78**: 044602.

[23] LIU F H. Europhys Lett, 2003, **63**: 193.

[24] LIU F H, ABD A N N, ZHANG D H, *et al*. Int J Mod Phys, 2003, **E12**: 713.

[25] LIU F H, ABD A N N, SINGH B K. Phys Rev, 2004, **C69**: 057601.

[26] LIU F H. Can J Phys, 2004, **82**: 109.

[27] LIU Fuhu. Nuclear Physics Review, 1998, **15**(1): 21(in Chinese).
(刘福虎. 原子核物理评论, 1998, **15**(1): 21.)

[28] LIU F H. Chin J Phys, 2001, **39**: 163.

[29] XIE Wenjie. Nuclear Physics Review, 2010, **27**: 274.

[30] XIE Wenjie, YANG De, WANG Cuiping, *et al*. Nuclear Physics Review, 2011, **28**(2): 179.

高能重离子碰撞中产生的末态粒子的横质量谱

谢文杰[1)]

(运城学院物理与电子工程系，山西 运城 044000)

摘要：基于多源理想气体模型，用两个方程分别描述了高能重离子中心碰撞中产生的 p，$K^{\pm}$ 和 $\pi^{\pm}$ 的横质量分布。在忽略末态粒子的相对论效应的情况下，除 $\pi^{\pm}$ 外，计算结果可近似地描述实验结果。考虑了源的次级样本后，发现计算结果与高能 Au-Au 和 Pb-Pb 中心碰撞的实验结果符合得较好。

关键词：多源理想气体模型；横质量谱；Au-Au 碰撞；Pb-Pb 碰撞

收稿日期：2011-03-02；**修改日期**：2011-04-17

基金项目：国家自然科学基金资助项目(10975095)；山西省自然科学基金资助项目(2007011005)

1) E-mail：wenjiexie@yeah.net